

# Analytical Utility of the Iridium-Based Mercury Ultramicroelectrode with Square-Wave Anodic Stripping Voltammetry

Samuel P. Kounaves\* and Wen Deng

Department of Chemistry, Tufts University, Medford, Massachusetts 02155

The characteristics of the iridium-based hemispherical mercury ultramicroelectrode (Hg-UME) in conjunction with square-wave anodic stripping voltammetry (SWASV) have been investigated. Using Hg-UMEs of 5–10- $\mu\text{m}$  radii, samples were analyzed without any added electrolyte, deoxygenation, or forced convection. The peak stripping currents displayed a linear relationship with deposition times varying from 1 to 1200 s. Peak potentials and current remained substantially unchanged with electrolyte concentrations of 1– $10^{-5}$  M. The reproducibility and useful lifetime of the Hg-UME was studied and found to be excellent over several days use. The application of SWASV theory for mercury film electrodes is shown to not entirely describe the response at the Hg-UME, especially at low square-wave frequencies.

## INTRODUCTION

The mercury electrode in its many forms has been the overwhelming substrate-of-choice for electrochemistry since the inception of polarography. The analytical utility of anodic stripping voltammetry (ASV) using mercury electrodes has been extensively developed during the past 20 years. In the past decade many attempts have been made to decrease the size of mercury electrodes to the micron range and to use them with fast-scan electroanalytical techniques for increased sensitivity and decreased analysis time.

Ultramicroelectrodes (UME) because of their size, typically less than 20  $\mu\text{m}$ , possess several very desirable characteristics in terms of such properties as transport rates, capacitive charging, and reduction in  $iR$  drop. These unique properties have helped them to rapidly become invaluable in a wide range of research areas and applications.<sup>1</sup> The most common materials used in their preparation have been platinum, gold, or carbon fibers, and their sizes have varied from 20 to 0.003  $\mu\text{m}$ .<sup>2–6</sup>

Several attempts have been made over the years at fabricating mercury UMEs (Hg-UME) both on solid substrates and in bulk form.<sup>7–12</sup> Pons and his group<sup>7</sup> constructed a dropping micro mercury electrode using a glass capillary

tubing with a small heated mercury reservoir in the center. Baars et al.<sup>12</sup> electrically “exploded” the orifice of a glass capillary, thereafter giving mercury drops of about 50- $\mu\text{m}$  radius. Even though these devices perform well for laboratory research work, they face many of the same problems that plague the classical DME or HMDE, especially for in situ environmental analytical work. In terms of plating mercury on a substrate to form a film or semisphere, Wehmeyer and Wightman<sup>8</sup> deposited mercury onto a platinum disk with a radius as small as 0.3  $\mu\text{m}$  and used it with ASV for the determination of lead in the concentration range  $7 \times 10^{-7}$  to  $1 \times 10^{-10}$  M. Baranski<sup>9</sup> prepared mercury film microelectrodes (7–10- $\mu\text{m}$  diameter) by deposition of mercury on carbon fiber or platinum wire and used them for rapid voltammetric determinations of trace metals in very small samples. Daniele et al.<sup>11</sup> used mercury deposited on a 1- $\mu\text{m}$ -diameter platinum UME to perform DP-ASV on various samples.

As in the case of millimeter-sized electrodes, the dissolution of a substrate such as Pt, Au, or Ag in the mercury and the resulting formation of intermetallic compounds with analyte metals deposited into the film can severely limit the long-term utility and theoretical behavior of such electrodes. This is especially true in studies utilizing ASV for speciation or in studies of electrode kinetics where even micromole fractions of metal impurities in the mercury can have significant effects on such parameters as the PZC of mercury.

Totally inert materials would of course be the most preferable substrates for mercury film/semisphere formation. The only commonly used material for UMEs with such properties has been carbon fiber. Unfortunately, its inertness also makes it difficult for the mercury to adhere to the surface and as a result the ruggedness, reproducibility, and practical utility of such Hg-UMEs suffers.<sup>7,9</sup>

Iridium has been shown to be an excellent substrate for the formation of a mercury film or semisphere.<sup>13–16</sup> Unlike platinum, gold, or silver, the solubility or iridium in mercury is well below 10<sup>-6</sup>% by weight.<sup>13,17</sup> Because iridium wire of less than 127- $\mu\text{m}$  diameter has not been commercially available, no reported attempts at fabricating an iridium-based mercury UME with a tip diameter in the micron or submicron range have been made until recently.<sup>18,19</sup> The properties of the mercury vis-à-vis the iridium surface (i.e.,

(1) Wightman, R. M.; Wipf, D. O. In *Electroanalytical Chemistry*; Bard, A. J., Ed.; Marcel Dekker: New York, 1989, Vol. 15, pp 267–353.

(2) Itaya, K.; Abe, T.; Uchida, I. *J. Electrochem. Soc.* 1987, 134, 1191–1193.

(3) Pendley, P. D.; Abruña, H. D. *Anal. Chem.* 1990, 62, 782–784.

(4) Singleton, S. T.; O’Dea, J. J.; Osteryoung, J. *Anal. Chem.* 1989, 61, 1211–1215.

(5) Penner, R. M.; Heben, M. J.; Lewis, N. S. *Anal. Chem.* 1989, 61, 1630–1636.

(6) Wightman, R. M. *Science* 1988, 240, 415–420.

(7) Pons, J.; Daschbach, J.; Pons, S.; Fleischmann, M. *J. Electroanal. Chem. Interfacial Electrochem.* 1988, 239, 427–431.

(8) Wehmeyer, K. R.; Wightman, R. M. *Anal. Chem.* 1985, 57, 1989–1993.

(9) Baranski, A. S. *Anal. Chem.* 1987, 59, 662–666.

(10) Wikiel, K.; Osteryoung, J. *Anal. Chem.* 1989, 61, 2086–2092.

(11) Daniele, S.; Baldo, M. A.; Ugo, P.; Mazzocchin, A. *Anal. Chim. Acta* 1989, 219, 9–18.

(12) Baars, A.; Sluyters-Rehbach, M.; Sluyters, J. H. *J. Electroanal. Chem. Interfacial Electrochem.* 1990, 283, 99–113.

(13) Kounaves, S. P.; Buffle, J. *J. Electrochem. Soc.* 1986, 133, 2495–2498.

(14) Kounaves, S. P.; Buffle, J. *J. Electroanal. Chem. Interfacial Electrochem.* 1987, 216, 53–69.

(15) Golas, J.; Galus, Z.; Osteryoung, J. *Anal. Chem.* 1987, 59, 389–392.

(16) Wechter, C.; Osteryoung, J. *Anal. Chem.* 1989, 61, 2092–2097.

(17) Guminski, C.; Galus, Z. In *Solubility Data Series—Metals in Mercury*; Hirayama, C., Guminski, C., Galus, Z., Eds.; Pergamon Press: Oxford, U.K., 1986; Vol. 25.

(18) Kounaves, S. P.; Deng, W. *J. Electroanal. Chem. Interfacial Electrochem.* 1991, 301, 77–85.

(19) DeVitre, R. R.; Tercier, M.-L.; Tscapoulos, M.; Buffle, J. *Anal. Chim. Acta* 1991, 249, 419–425.

surface tension and energy) favor the formation of a more stable well-adhering mercury hemisphere at the micrometer-sized iridium disk than would have been predicted from the previous experiences<sup>13-16</sup> with the macro iridium-based mercury film electrodes.

In this paper we describe the use of the Ir-based Hg-UME with square-wave anodic stripping voltammetry for the analysis of copper, cadmium, and lead at concentrations of  $10^{-5}$  to  $10^{-9}$  M in various types of water samples, without intentionally added electrolyte, with various concentrations of intentionally added electrolyte, with no stirring during the deposition step, and with no deoxygenation. In addition we examine the behavior of the peak current response with SW frequency and look at SWASV theory for the mercury film electrode (MFE) as applied to the hemispherical Hg-UME.

## EXPERIMENTAL SECTION

**Reagents.** All solutions were prepared with 18-M $\Omega$  deionized water from a Barnstead Nanopure system (Barnstead Co., Newton, MA). Buffer solutions were prepared from 99.99+ % ammonium acetate and acetic acid, and the pH was adjusted to 4.5 with addition of HClO<sub>4</sub> (Aldrich). Metal solutions were prepared from 99.9995% Cu(NO<sub>3</sub>)<sub>2</sub>, Cd(NO<sub>3</sub>)<sub>2</sub>, Zn(NO<sub>3</sub>)<sub>2</sub>, Hg<sub>2</sub>(NO<sub>3</sub>)<sub>2</sub> (ALFA-Johnson Matthey, Ward Hill, MA), and Pb(NO<sub>3</sub>)<sub>2</sub> (Aldrich). All other solutions were prepared from ACS reagent grade chemicals. The nitrogen gas used was ultra-high-purity grade (Northeast Airgas, Inc.) passed through an oxygen adsorbing filter (OxiClear, VWR Scientific, Boston, MA).

**Apparatus.** Square-wave anodic stripping voltammetry was performed using either an EG&G PAR Model 273 potentiostat/galvanostat (EG&G PAR, Princeton, NJ) interfaced to an IBM PS/2-30286 with custom control software or a CYSY-1090 computer-controlled electroanalysis system (Cypress Systems, Lawrence, KS). All voltammetric experiments were performed using a two-electrode system consisting of the working UME and reference electrode with the entire cell enclosed in a Faraday cage. Optical in situ microscopic observations of the electrodes were made with a Metaval-H (Leco/Jena) inverted polarizing microscope equipped with a video imaging processing system and a 35-mm Pentax camera for microphotography.

**Reference Electrodes.** The use of UMEs allows SWASV measurement to be conducted with very little or no added supporting electrolyte. Under these conditions it is very important for the reference electrode itself not to introduce any significant amount of electrolyte into the sample. The commonly used saturated calomel reference electrodes contain a liquid internal electrolyte and a fiber or Vycor junction which can leak significant amounts of Cl<sup>-</sup>, even when a sample-filled bridge is used. To overcome this leakage problem, we have fabricated and used a custom-made solid-state Nafion-coated Ag/AgCl reference electrode (SSNE) containing no internal liquid electrolyte or flow junctions.<sup>20</sup> Unless otherwise indicated, all potentials are versus the SSNE (approximately +220 mV vs SCE). The exception to this was the use of a sodium-saturated calomel reference electrode (SSCE) for deposition of the mercury hemisphere on the iridium substrate.

**Preparation of the Iridium-Based Ultramicroelectrode.** The iridium-based mercury UME was prepared as described previously.<sup>18</sup> The iridium wire was etched in a molten salt bath composed of a 6 to 1 by weight mixture of NaNO<sub>3</sub> and NaCl at 445 °C with a 100-Hz sine-wave of 1.0 V (rms) applied between the immersed Ir wire and the Pt crucible containing the molten salt mixture. The Ir wire was then placed into a glass capillary pipet and the etched end sealed into the capillary by melting the glass. The other end of the iridium wire was twisted around a solid copper wire and brazed using a silver alloy. The entire assembly, except for several millimeters at the tip, was made ridged by covering with heat-shrinkable tubing. The tip was then ground flat using a high-speed rotating wheel with 600- and 1200-grit silicon carbide (CARBIMET, Buehler Ltd., Lake Bluff, IL) and successively hand polished with 1.0-, 0.3-, and 0.05- $\mu$ m

alumina (MICROPOLISH, Buehler Ltd.). Each electrode was also electrochemically characterized as previously described to assure a defect-free glass/iridium seal.<sup>18</sup>

The mercury hemisphere was formed by coulometric deposition at -0.2 V vs SSCE in a solution containing  $8 \times 10^{-3}$  M Hg(II) and 0.1 M HClO<sub>4</sub>. The geometry of the deposited mercury can be controlled from a thin film to almost a sphere depending on the deposition parameters.<sup>18</sup> Because of its ruggedness and stability the hemispherical geometry was used for all analyses. As in previous studies, the deposition charge was normally used to determine coverage of the substrate.<sup>8,14,18</sup> Typically, for an electrode with a radius of approximately 6.5  $\mu$ m, a charge of 30  $\mu$ C resulted in a hemispherical coverage. This value was frequently verified by microscopic observation to assure a true hemispherical geometry. For optimum performance the mercury was replated at the beginning of each day even though when stored in deionized water with application of a slight negative potential it could be maintained for several days. After deposition of mercury, the electrode was removed from the Hg(II) solution, rinsed carefully with deionized water, and then transferred to the sample cell. A unique and useful advantage of the Ir-based Hg-UME is that, if one so desires, the Hg hemisphere can be completely removed from the surface by simply applying a potential of +600 mV.

Because of the unique UME characteristics of high mass transport and the steady-state diffusional flux, the sample solutions were kept quiescent during the preconcentration and no equilibration period was needed before initiating the anodic scan. Unless otherwise indicated, SWASV measurements were carried out with a SW amplitude of 25 mV, a SW step height of 5 mV, and a SW frequency of 150 Hz.

## RESULTS AND DISCUSSION

Some of the excellent characteristics found in several previous studies with macro iridium-based mercury electrodes<sup>14-16</sup> have been further confirmed in this study. The analytical results for this electrode were found to be better than or comparable to those obtained with other types of mercury microelectrodes<sup>8,9</sup> but with the advantage of a stable mercury hemisphere and no intermetallic compound formation between the iridium substrate and the metal analytes.

**Peak Current vs Deposition Time.** Calculations indicated that under the conditions used here, the concentrations of the deposited metals (Cu, Cd, and Pb) would not exceed their solubility limits in the mercury hemisphere during the deposition step. However, experimental confirmation of linear behavior is important with new types of mercury ultramicroelectrodes, demonstrating that the solubility of the analyte metal in the mercury is indeed not exceeded. The dependency of the SWASV peak stripping current ( $i_p$ ) on the deposition time ( $t_d$ ) was evaluated using a 6.5- $\mu$ m radius Hg-UME with  $1 \times 10^{-7}$  M Pb<sup>2+</sup> and Cd<sup>2+</sup> in 0.2-0.002 M acetate buffer (pH4.5) or 0.1-0.001 M NaClO<sub>4</sub>. The square-wave parameters used were  $E_{sw} = 25$  mV,  $E_s = 5$  mV, and  $f = 150$  Hz. The depositions were made at a potential of -1400 mV with the deposition time ranging from 10 to 600 s. As shown in Figure 1, for deposition times greater than about 50 s the peak stripping current increases linearly with deposition time for both electrolytes, and removal of dissolved O<sub>2</sub> by purging with N<sub>2</sub> had no significant effect on the slope or peak current. The same behavior was also noted with the other concentrations of electrolyte.

**Effects of Electrolyte Concentration.** The effects of electrolyte concentration were studied using a 6.5- $\mu$ m-radius Hg-UME, with  $1 \times 10^{-7}$  M Cd<sup>2+</sup> and  $1 \times 10^{-7}$  M Pb<sup>2+</sup> in 1-10<sup>-7</sup> M NaClO<sub>4</sub> and deposition times of 60-240 s ( $E_{sw} = 25$  mV,  $E_s = 5$  mV,  $f = 150$  Hz). The peak SWASV current for both Cd<sup>2+</sup> and Pb<sup>2+</sup> remained basically unchanged over the entire range of concentrations. The peak potential ( $E_p$ ) was also relatively constant over the entire concentration range except for a small anodic shift of about 8 mV between 10<sup>-1</sup> and 10<sup>-3</sup>

(20) Deng, W.; Kounaves, S. P. Manuscript in preparation.

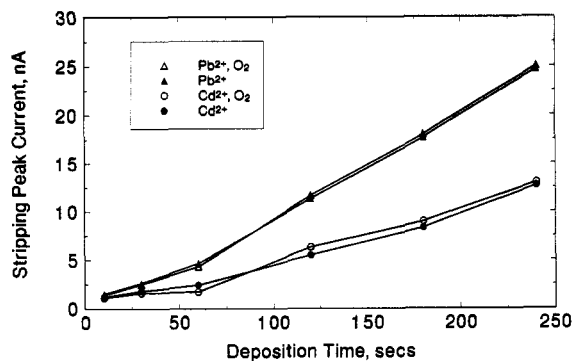


**Figure 1.** Effect of deposition time on SWASV peak current for  $1 \times 10^{-7}$  M  $\text{Pb}^{2+}$  and  $\text{Cd}^{2+}$  in 0.1 M  $\text{NaClO}_4$  with and without deoxygenation of sample. SWASV parameters:  $E_{sw} = 25$  mV,  $E_s = 5$  mV,  $f = 150$  Hz,  $r = 6.5$   $\mu\text{m}$ .

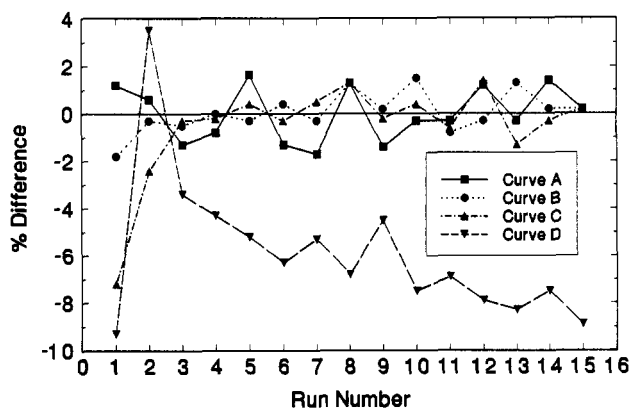


**Figure 2.** Evaluation of Hg-UME performance over several days. Percent difference compared to initial 15 runs after (A) 0 h, (B) 5 h, (C) 28 h, and (D) 52 h. Conditions:  $E_{sw} = 25$  mV,  $E_s = 5$  mV,  $f = 150$  Hz,  $T_d = 60$  s,  $r = 6.5$   $\mu\text{m}$ ,  $1 \times 10^{-7}$  M  $\text{Pb}^{2+}$  in 0.01 M  $\text{NaClO}_4$ .

M. This anodic shift may be due to the increased effects of migration control over diffusion control. Removal of dissolved  $\text{O}_2$  by purging with  $\text{N}_2$  had no significant effect on either the peak current or potential.

**Reproducibility and Useful Lifetime.** As mentioned above, the Hg-UME was cleaned with concentrated nitric acid and replated with mercury at the beginning of each days work. There were cases in which the Hg-UME had been left sitting in deoxygenated deionized water for more than 1 week and was found to be still capable of giving good analytical results. There were also a few rare cases where the electrode appeared to deteriorate after only a couple of hours of use in the same type of solution. Figure 2 shows a quantitative voltammetric evaluation of the Hg-UMEs performance with SWASV by taking 15 consecutive runs at several points over several days. A 6.5- $\mu\text{m}$ -radius Hg-UME was used with  $1 \times 10^{-7}$  M  $\text{Pb}^{2+}$  in 0.01 M  $\text{NaClO}_4$  and a deposition time of 60 s. The y-axis shows the percent difference of the peak current, where the 0% line is the average current for 15 consecutive runs (i.e., SWASV experiments). The first 15 runs (curve A) show an excellent reproducibility for SWASV analysis at the Hg-UME of  $\pm 2\%$ . Curve B shows an additional 15 consecutive runs made 5 h later with the 0% difference being in respect to the first set of runs (curve A). There appears to be a small determinate negative difference for the first couple of runs, but it quickly returns to an indeterminate  $\pm 2\%$ . Curve C shows the same procedure carried out 23 h later (28 h from start). In this case the first two runs show a substantial decrease in peak current ( $-8\%$  and  $-2.5\%$ ) before the previous reproducibility is reestablished. Finally, after another 24 h (52 h from start) we observe in curve D the results of an irreversibly deteriorated Hg-UME surface. For this last set, only the second run gave a reasonable SWASV peak current,

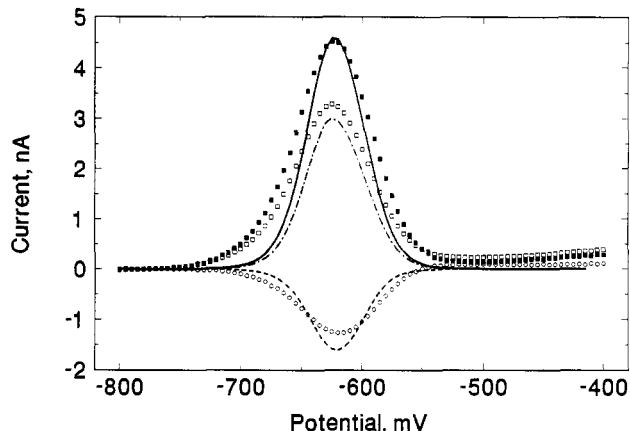


**Figure 3.** Theoretical (---) and experimental forward ( $\square$ ), reverse ( $\circ$ ) and net ( $\blacksquare$ ) SW anodic stripping voltammogram of  $10^{-7}$  M  $\text{Cd}^{2+}$  in 0.01 M  $\text{KNO}_3$ , with  $E_{sw} = 25$  mV,  $E_s = 5$  mV,  $f = 150$  Hz,  $T_d = 10$  s, and  $r = 10$   $\mu\text{m}$ .

while the remaining runs went from about 3% negative difference to about 9% difference by the 15th run.

Microscopic examination of the Hg-UME surface showed only a mirrorlike hemisphere for the data shown in the first three curves of Figure 2. The surface observed, before the data in curve C was taken, showed partial coverage of the mercury surface by some type of particulate film. This "film" may be due to either  $\text{HgO}$  formation from  $\text{O}_2$  in solution or  $\text{HgCl}$  from trace  $\text{Cl}^-$  impurities in the electrolyte. There were some cases however in which electrochemical behavior was perturbed even though no surface deterioration could be seen and some cases in which some film coverage was visible on the Hg-UME surface but response was satisfactory.

**Application of SWASV-MFE Theory to the Hg-UME.** There is at present no complete theoretical model for the response of SWASV at a hemispherical mercury ultramicroelectrode. However, existing theoretical treatments for SWASV of mercury-soluble metal ions at the MFE<sup>21,22</sup> and SWV at solid ultramicroelectrodes<sup>23</sup> should be applicable to the hemispherical Hg-UME under certain limiting conditions.

Figure 3 shows a typical experimental forward ( $\square$ ), reverse ( $\circ$ ), and net ( $\blacksquare$ ) SW anodic stripping voltammogram of  $10^{-7}$  M  $\text{Cd}^{2+}$  in 0.01 M  $\text{KNO}_3$  (with  $E_{sw} = 25$  mV,  $E_s = 5$  mV,  $f = 150$  Hz,  $T_d = 10$  s,  $r = 10$   $\mu\text{m}$ ). The accompanying theoretical curves (---), for the exact same conditions (letting  $l = r = 8$   $\mu\text{m}$ , and  $\Lambda = l\sqrt{f/D_R} = 3.2$ ) using SWASV theory at the MFE,<sup>21</sup> were normalized only in terms of peak height in order to fit the experimental data. This is necessary since conversion of the theoretical current function value ( $\psi$ ) to a real current would require knowing the exact charge and/or concentration of the metal in the mercury. The fit appears to be rather close except for the peak width at half-height ( $W_{1/2}$ ), which is 70 mV for the experimental and 58 mV for the theoretical data. This discrepancy between SWASV-MFE theory and the experimental data (which was present for all of the SWASV experiments) most likely arises from trying to equate the mercury film thickness with the hemispherical mercury radius. The occurrence of wider ASV peaks has also been previously noted with LSASV at the MFE,<sup>24</sup> with SWASV at a Ag-based MFE,<sup>10</sup> and at a micro-MFE array.<sup>25</sup> In all

(21) Kounaves, S. P.; O'Dea, J. J.; Chandrasekhar, P.; Osteryoung, J. *Anal. Chem.* 1987, 59, 386-389.

(22) Penczek, M.; Stojek, Z. *J. Electroanal. Chem. Interfacial Electrochem.* 1986, 213, 177-185.

(23) Whelan, D.; O'Dea, J. J.; Osteryoung, J.; Aoki, K. *J. Electroanal. Chem. Interfacial Electrochem.* 1986, 202, 23-36.

(24) Kounaves, S. P.; Buffle, J. *J. Electroanal. Chem. Interfacial Electrochem.* 1988, 239, 113-123.

(25) Ciszowska, M.; Stojek, Z. *J. Electroanal. Chem. Interfacial Electrochem.* 1985, 191, 101-111.

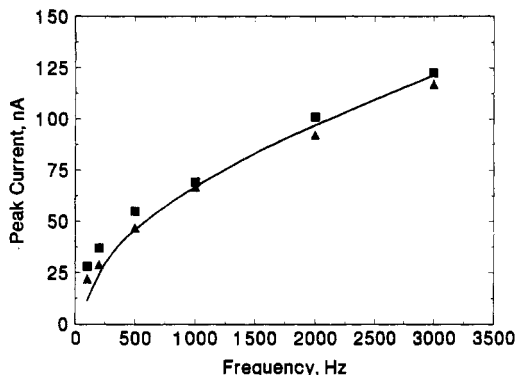


**Figure 4.** Theoretical (—) and experimental (▲, ■) behavior of  $i_p$  as a function of SW frequency at two different electrolyte concentrations. Conditions:  $10^{-7}$  M  $Pb^{2+}$  in 1.0 and 0.001 M acetate buffer (pH 4.5), with  $E_{sw} = 25$  mV,  $E_s = 5$  mV,  $T_d = 60$  s, and  $r = 10$   $\mu$ m.

these cases the mercury film was actually a spherical segment as opposed to a mercury film of uniform thickness. It is apparent from the results obtained in this study and from some recent preliminary derivations for the theory of SWASV at a hemispherical mercury UME<sup>26</sup> that the MFE theory may underestimate the peak width for the hemispherical case. However, in spite of this divergence, the theory for the MFE provides a reasonable approximation for the expected behavior of SWASV at the hemispherical Hg-UME.

**Peak Current Dependency on SW Frequency.** Keeping the above points in mind, the theory for SWASV at a mercury film electrode<sup>21</sup> was used to provide a prediction for  $i_p$  as a function of the square-wave frequency ( $f$ ) at different electrolyte concentrations. Assuming an "average" mercury film thickness ( $l$ ) of 5  $\mu$ m for a hemispherical Hg-UME with a radius of 6.5  $\mu$ m,  $i_p$  was calculated from SWASV/MFE theory using the equation

$$i_p = \psi_p n F A C_R^* \sqrt{D_{Rf}/\pi} \quad (1)$$

where  $\psi_p$  is the numerically calculated dimensionless current function,  $C_R^*$  is the initial homogeneous concentration of the analyte metal in the mercury film (hemisphere), and the other symbols have their usual meanings.

Figure 4 shows the theoretical (—) and experimental (▲, ■) behavior of  $i_p$  as a function of SW frequency at two different electrolyte concentrations. The experimental data were obtained using a 6.5- $\mu$ m-radius Hg-UME in 1.0 and 0.001 M acetate buffer (pH 4.5) containing  $1 \times 10^{-7}$  M  $Pb^{2+}$  with a deposition time of 60 s, and all other conditions were the same as above. Even though some previous studies have shown nontheoretical behavior of  $i_p$  with  $f$  for mercury electrodes,<sup>27</sup> the results obtained here for the hemispherical Hg-UME show a reasonably good fit between theory and experiment for  $30 < f < 3000$  Hz and with only a slight difference between electrolyte concentrations. Similar results were also obtained with  $NaClO_4$ , for other electrolyte concentrations, different metals, and different deposition times. For  $30 < f < 1000$  Hz and for all electrolyte concentrations studied, the shapes of the individual SW voltammograms were similar to those calculated from SWASV-MFE theory,<sup>21</sup> but the peak currents were 10–20% greater than predicted (Figure 4). On the other hand, for  $1000 < f < 3000$  Hz, the peak currents appeared to follow theory, but the peaks were 20–25% wider than predicted. These data suggest that at lower SW frequencies SWASV at the Hg-UME is not fully modeled by the SWASV-MFE theory. Indeed, this might be expected since at lower frequencies there is enough time for

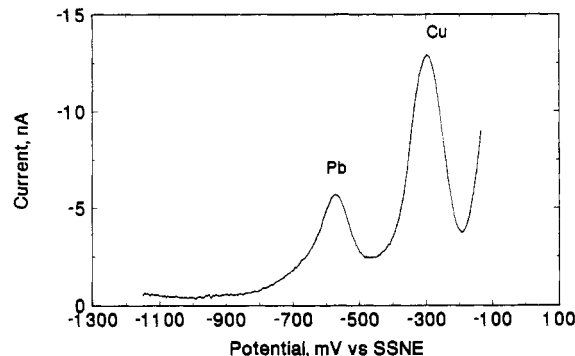


**Figure 5.** SWASV analysis for  $Pb^{2+}$  and  $Cu^{2+}$  in unmodified drinking water at a Hg-UME with  $E_{sw} = 25$  mV,  $E_s = 5$  mV,  $f = 680$  Hz,  $T_d = 300$  s,  $r = 6.5$   $\mu$ m.

a substantial spherical diffusion layer to develop at the Hg-UME, thus increasing radial mass transport. At higher frequencies the diffusion layer becomes much thinner relative to the size of the hemisphere and the behavior approaches that for linear diffusion at the MFE.

**Analysis of Environmental Samples.** The ability to use UMEs in solutions whose concentrations of supporting electrolyte are no greater than those of the analytes, but behave as "excess" supporting electrolyte,<sup>28</sup> makes them ideal for analysis of metal ions in natural waters or solutions where added electrolyte is not desirable. Their high mass transport rate eliminates the need for stirring during the deposition step, and when used with SWASV, the fast scan rate and irreversibility of  $O_2$  reduction eliminates the need to deoxygenate the solution. We have used the Ir-based Hg-UME in conjunction with SWASV to determine trace heavy metals such as  $Pb^{2+}$  and  $Cu^{2+}$  in drinking water, lake water, sea water, and various model buffer systems. For all the natural water samples there was no intentionally added electrolyte, deoxygenation, or stirring during the preconcentration step. In addition to the advantages of the iridium substrate and SWASV, the results of our work support the excellent reproducibility and precision demonstrated by several previous studies of mercury UMEs.<sup>8,9,18,19</sup>

As an example, Figure 5 shows the utility of the Hg-UME with SWASV for the determination of  $Pb^{2+}$  and  $Cu^{2+}$  in unmodified drinking water at a Hg-UME (with  $E_{sw} = 25$  mV,  $E_s = 5$  mV,  $f = 680$  Hz,  $T_d = 300$  s,  $r = 6.5$   $\mu$ m). The lead and copper SWASV peaks are sharp, well defined, without any distortion. The standard addition curve was linear and gave a  $Cu^{2+}$  and  $Pb^{2+}$  concentration in the drinking water of  $(1.5 \pm 0.3) \times 10^{-6}$  and  $(1.1 \pm 0.3) \times 10^{-8}$  M, respectively.

The detection limit for SWASV at a Hg-UME is of course dependent on the length of the deposition time and square-wave frequency. However, it is interesting to note that the detection limit does not appear to vary with either electrolyte concentration or the presence/absence of  $O_2$  in the sample. For a Hg-UME of 6.5- $\mu$ m radius, in 0.002 M acetate buffer (pH 4.5), the detection limit for both Cu and Pb was  $1 \times 10^{-6}$  M for  $T_d = 0$  s,  $1 \times 10^{-8}$  M for  $T_d = 120$  s, and  $1 \times 10^{-9}$  M for  $T_d = 240$  s.

The precision of SWASV at the Hg-UME was determined using  $1 \times 10^{-7}$  M  $Pb^{2+}$  and  $Cu^{2+}$  in 0.001 M acetate buffer. The relative deviation for 10 measurements was 2.8% and 3.9% for Pb and Cu, respectively.

## CONCLUSIONS

The combination of an Ir-based mercury ultramicroelectrode with square-wave anodic stripping voltammetry pro-

(26) Liu, Z.; Kounaves, S. P. Unpublished work.

(27) Kounaves, S. P.; Deng, W. *J. Electroanal. Chem. Interfacial Electrochem.* 1991, 306, 111–124 and references therein.

(28) Oldham, K. B. *J. Electroanal. Chem. Interfacial Electrochem.* 1988, 250, 1–21.

vides a rapid, accurate, and sensitive method for the determination of metal ions in aqueous solutions without deoxygenation, any intentionally added electrolyte, or stirring during the deposition step. The mercury is well adhering and stable for long periods of time, with no indication of amalgam formation. Peak stripping currents displayed a linear relationship with deposition times varying from 1 to 1200 s and indicated the lack of any intermetallic compound formation in the mercury. Peak potentials and current remained substantially unchanged with electrolyte concentrations of  $1-10^{-5}$  M. The reproducibility and useful lifetime of the Hg-UME was studied and found to be excellent over several days of use. The behavior of the stripping peak current does not appear to be adequately modeled by SWASV theory for the MFE, and we are currently working on a theoretical

model for a more complete description of SWASV at the hemispherical Hg-UME.

#### ACKNOWLEDGMENT

This work was supported in part by Grants from the U.S. Environmental Protection Agency through the Northeast Hazardous Substance Research Center and the Tufts Center for Environmental Management. The information contained in this document does not necessarily reflect the views of the Agency or the Centers, and no official endorsement should be inferred.

RECEIVED for review August 3, 1992. Accepted November 19, 1992.